



Sputtering studies of beryllium with helium and deuterium using molecular dynamics approach

Shuzo Ueda^{a,*}, Toshiro Ohsaka^b, Satoru Kuwajima^c

^a Department of Fusion Plasma Research, Naka Fusion Research Establishment, Japan Atomic Energy Research Institute, Naka-machi, Naka-gun, Ibaraki 311-0193, Japan

^b Applied Engineering Department, Science and Engineering Division, CRC Research Institute, Inc., 2-7-5 Minamisuna, Koto-ku, Tokyo 136-8581, Japan

^c NanoSimulation Associates, 825-1 Amado-cho, Villa D.E. 201, Hanamigawa-ku, Chiba-shi, Chiba 262-0043, Japan

Abstract

The Be sputtering with He and D was simulated by a molecular dynamics (MD) approach with the use of newly developed He–Be and H–Be (or D–Be) interatomic potentials. The H–Be potential incorporates many-body effects through the implementation of the Tersoff potential. A modification was introduced in the Tersoff potential in order to adapt it to the sputtering simulation. Incident angle dependence of the sputtering was examined at the incident particle energy of 100 eV with respect to the crystal surface (0 0 1), (0 1 0) and (1 1 0) for the He bombardment and (0 0 1) for the D bombardment. The calculated sputtering yields and reflection coefficients are in reasonable agreement with the TRIM.SP evaluations. Surface dependence is clearly observed in the He bombardment. The MD sputtering yield and reflection coefficient become significantly reduced at grazing angles and significantly enhanced than the TRIM.SP evaluations, respectively. © 2000 Elsevier Science B.V. All rights reserved.

1. Introduction

Atomic scale computer simulations are gaining ground in the study of fusion reactor materials [1]. As an effort in this trend, the authors have been pursuing a sputtering study of Be, a candidate plasma facing material, by using atomistic molecular dynamics (MD) approach. In a previous paper [2], hereafter referred to as I, the self-sputtering was investigated. In the present paper, we extend the work to the Be sputtering with He and D.

Interatomic potentials are of vital importance in atomistic simulations of materials. In paper I, we developed a Be–Be interaction potential suitable for the sputtering simulation. In the present paper, we have to develop He–Be and H–Be (or D–Be) potentials. While

the He–Be interaction is easily handled by using a simple 2-body potential, the H–Be interaction poses a challenge because of its many-body nature. Thus, a central part of our efforts consists of the development of an H–Be many-body potential adapted to the sputtering simulation. By using the newly developed potentials, we have carried out sputtering simulations examining angle dependence of the sputtering yield and reflection coefficient. We also investigate the surface (crystal face) dependence of the sputtering yield for the case of the He–B sputtering.

2. He–Be interatomic potential

We start with the construction of a potential for the He–Be interaction. This interaction should be well approximated by a 2-body potential because of the inert nature of the He atom. We adopt the standard Moliere function [3] to represent the interaction

$$u_{\text{BeHe}}(r) = (8e^2/r)\phi(r/a_{\text{BeHe}}), \quad (1)$$

* Corresponding author. Present address: Office of Foreign Affairs, Japan Atomic Energy Research Institute, Baumannstrasse 4/2/13, A1030 Vienna, Austria. Tel.: +43-1 713 0751; fax: +43-1 713 0753.

E-mail address: wien@hems.jaeri.go.jp (S. Ueda).

where r denotes the interatomic distance, a_{BeHe} an adjustable parameter, e the elementary charge, and ϕ is defined by

$$\phi(x) = 0.35 \exp(-0.3x) + 0.55 \exp(-1.2x) + 0.1 \exp(-6x). \quad (2)$$

Potential (1) is purely repulsive in contrast to our Be–Be potential (paper I) that is composed of a Moliere term and an attractive function.

The adjustable parameter has been determined as $a_{\text{BeHe}} = 0.1597$ (Å) through the fitting of ab initio quantum chemical potentials. The RHF level of theory with a contracted Gaussian basis set of Chiles and Dykstra [4,5] was applied to the BeHe system by using a software package SPARTAN [6].

3. H–Be interatomic potential

3.1. Potential function

As stressed in Section 1, construction of an H–Be many-body potential suitable for the sputtering simulations is a central task of the present paper. Since the many-body character of the H–Be interactions comes from the covalent nature of the H–Be bond, we adopt the Tersoff potential [7] which is a standard potential to model many-body interactions caused by covalent bonds. As the Tersoff potential by itself does not provide enough degrees of freedom to mimic ab initio quantum chemical potential surface, we have added a Moliere-type function and an exponential function to the 2-body part of the H–Be interaction. Thus, the potential U is represented as

$$U = E_{\text{Tersoff}} + E_{2\text{-body}}. \quad (3)$$

Noting that sputtering simulations involve just one H (or D) atom, the 2-body part is written as

$$E_{2\text{body}} = \sum_j^{\text{Be}} [(4e^2/r_{\text{Hj}})\phi(r_{\text{Hj}}/a_{\text{HBe}}) - w_{\text{HBe}} \exp(-r_{\text{Hj}}/d_{\text{HBe}})] + \sum_{j<k}^{\text{Be}} u(r_{jk}), \quad (4)$$

where the summation runs over Be atoms, r_{Hj} the distance between the H atom and j th Be atom, and $u(r)$ denotes the Be–Be interaction potential defined in paper I.

The Tersoff potential in the present case of Be_nH systems takes the form [7]

$$E_{\text{Tersoff}} = E_{\text{H}} = \sum_j^{\text{Be}} V_{\text{Hj}}, \quad (5)$$

where the H–Be interaction potential V_{Hj} is given by

$$V_{\text{Hj}} = f_{\text{C}}(r_{\text{Hj}})[f_{\text{R}}(r_{\text{Hj}}) + b_{\text{Hj}}f_{\text{A}}(r_{\text{Hj}})]. \quad (6)$$

The functions f_{R} and f_{A} in Eq. (6) represent the repulsive and attractive part of the potential, respectively. The function f_{C} is a switching function that smoothly reduces the potential to zero outside the covalent region

$$f_{\text{C}}(r) = \begin{cases} 1 & (r < R), \\ 0.5\{1 + \cos[\pi(r - R)/S - R]\} & (R \leq r \leq S), \\ 0 & (r > S). \end{cases} \quad (7)$$

Many-body effects of the Tersoff potential are embodied by the factor b_{Hj} of Eq. (6). This factor is written as

$$b_{\text{Hj}} = \chi_{\text{HBe}} (1 + \beta_{\text{H}}^n \zeta_{\text{Hj}}^n)^{-1/2n_{\text{H}}}, \quad (8)$$

where χ_{HBe} , n_{H} , and β_{H} are constants and

$$\zeta_{\text{Hj}} = \sum_{k \neq j}^{\text{Be}} f_{\text{C}}(r_{\text{Hk}}) \omega_{\text{HBe}} g_{\text{H}}(\theta_{\text{Hjk}}), \quad (9)$$

with ω_{HBe} being a constant. The $g_{\text{H}}(\theta_{\text{Hjk}})$ function is given by

$$g_{\text{H}}(\theta_{\text{Hjk}}) = 1 + c_{\text{H}}^2/d_{\text{H}}^2 - c_{\text{H}}^2/[d_{\text{H}}^2 + (h_{\text{H}} - \cos \theta_{\text{Hjk}})^2], \quad (10)$$

where c_{H} , d_{H} , and h_{H} are constants and θ_{Hjk} denotes the j – H – k angle.

In applying the above expressions, we make further simplifications. First, the angle dependence of the ζ factor, Eq. (9), is ignored: i.e., the g_{H} function, Eq. (10), is taken to be a constant (unity). We also fix the parameters χ_{HBe} , n_{H} , and ω_{HBe} to unity following the Tersoff paper [7]. Then the remaining adjustable parameter is only β_{H} . Thus, the b factor, Eq. (8), in the present case is reduced to the form

$$b_{\text{Hj}} = \left[1 + \beta_{\text{H}} \sum_{k \neq j}^{\text{Be}} f_{\text{C}}(r_{\text{Hk}}) \right]^{-1/2}. \quad (11)$$

We have not yet specified the functional form of f_{R} and f_{A} in Eq. (6). In the original Tersoff paper [7], exponential functions were used, i.e.,

$$f_{\text{R}}(r) = A \exp(-\lambda r), \quad f_{\text{A}}(r) = -B \exp(-\mu r). \quad (12)$$

However, we have found that Eqs. (12) is inappropriate for sputtering simulations (see Section 5). Instead, we have adopted the following form for the attractive potential:

$$f_{\text{A}}(r) = -B \exp(-\mu r) / [1 + (B/\varepsilon) \exp(-\mu r)]. \quad (13)$$

Note that this function is reduced to the original Tersoff form if $B \ll \varepsilon$. The repulsive function f_{R} is chosen so that the sum of the repulsive and attractive parts is the same as that in the original Tersoff formalism. Thus, we obtain

$$f_R(r) = A \exp(-\lambda r) - (B^2/\varepsilon) \exp(-2\mu r) / [1 + (B/\varepsilon) \exp(-\mu r)]. \quad (14)$$

In summary our interaction potential for Be_nH systems is defined by Eqs. (3)–(7), (11), (13) and (14). The values of the parametric constants appearing in these expressions are listed as follows: $a_{\text{HBe}} = 0.2252$ (Å), $w_{\text{HBe}} = -1.9414$ (eV), $d_{\text{HBe}} = 1.0335$ (Å) [Eq. (4)], $R = 0.0$, $S = 3.2$ (Å) [Eq. (7)], $\beta_H = 0.968$ [Eq. (11)], $B = 721.37$ (eV), $\mu = 1.5240$ (Å⁻¹), $\varepsilon = 40$ (eV) [Eq. (13)], $A = 751.32$ (eV), $\lambda = 1.6097$ (Å⁻¹) [Eq. (14)].

3.2. Parameter fitting

The parameters above are basically determined by using ab initio quantum chemical potentials as the reference. We calculated BeH and Be₂H systems with the RHF/6-311G** level of theory. In the case of the BeH diatomic system the total potential U , Eq. (3), is reduced to

$$U(r) = f_C(r)[A \exp(-\lambda r) - B \exp(-\mu r)] + (4e^2/r)\phi(r/a_{\text{HBe}}) - w_{\text{HBe}} \exp(-r/d_{\text{HBe}}), \quad (15)$$

where r denotes the interatomic distance. While all the parameters involved in Eq. (15) can be determined from the quantum chemical BeH potentials, the Moliere parameter a_{HBe} has been assigned the standard theoretical value [3]. (This is because we could not obtain the quantum chemical potentials at distances shorter than 0.4 Å.) The parameters A , λ , B , μ , w_{HBe} , and d_{HBe} have been determined by the least-squares fit of the quantum chemical potentials. As for the R and S parameters contained in the f_C function [Eq. (7)], they were selected on a trial and error basis without performing a full least-squares fit. The quantum chemical potentials and the fitting potentials from Eq. (15) are shown in Fig. 1.

The remaining parameters, β_H and ε , were determined from the Be₂H triatomic system in linear geometry. The position of each atom was (0, 0, 0) for the H atom, (-1.3426 Å, 0, 0) for one Be atom, and (r , 0, 0) for the other Be atom with r being a variable. (1.3426 Å is the equilibrium distance of the BeH molecule within the RHF/6-311G** theory.) The total potential (3) in this system becomes

$$U(r) = f_C(r)\{f_R(r) + [1 + \beta_H f_C(r_e)]^{-1/2} f_A(r)\} + f_C(r_e)\{f_R(r_e) + [1 + \beta_H f_C(r)]^{-1/2} f_A(r_e)\} + E_{2\text{-body}}, \quad (16)$$

where r_e is 1.3426 Å. Least-squares calculations were done on $0.5 \text{ \AA} \leq r \leq 3.2 \text{ \AA}$. We did not perform the full least-squares fitting with respect to the ε parameter. Instead, we fixed ε at 20, 30, 40, 50, and 70 eV and carried out the least-squares calculations for β_H . The best ε value

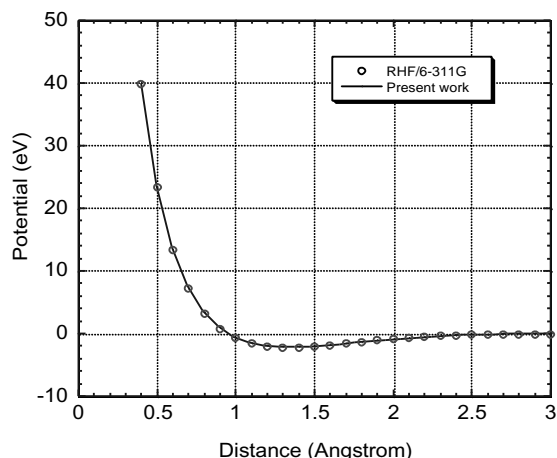


Fig. 1. A comparison of potential of the BeH system between ab initio and fitting potentials.

Table 1
Target crystal and incident energy

Incident atom	Crystal size (nm) ^a	No. of atoms	Face
D	2.02 × 1.94 × 2.76	1440	(0 0 1)
He	2.02 × 1.94 × 2.76	1440	(0 0 1)
He	2.47 × 2.58 × 23.3	1925	(0 1 0)
He	2.58 × 23.3 × 23.6	1848	(1 1 0)

^aThe size of the initial structure is listed. The z -length is the thickness of the crystal plate.

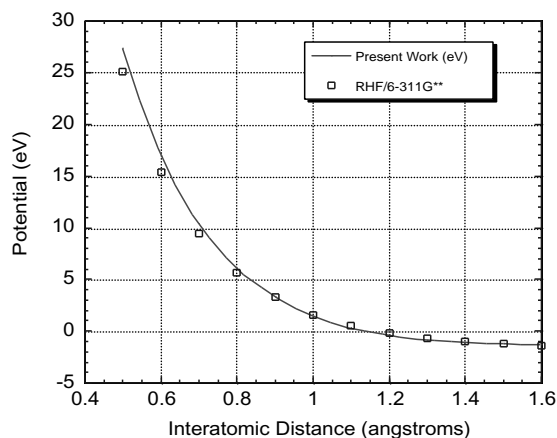


Fig. 2. A comparison of potential of the Be₂H system between ab initio and fitting potentials.

among them is selected in Table 1. The comparison of the RHF/6-311G** potential and the potential from Eq. (16) is shown in Fig. 2.

3.3. Parameter verification

We performed additional quantum chemical calculations for the Be_2H system in order to check the validity of our potential. A total of 25 geometries were searched, the atom coordinates being $(\pm 1.122, 0, 0)$ for the Be atoms and $(0.1683m, 0.1122n, 0)$ for the H atom ($m, n = 0, 1, 2, 3, 4$). The separation of the Be atoms, 2.244 Å, corresponds to the nearest-neighbor distance in the hcp crystal [2]. The root mean-square deviation over the 25 points, where the potential varies by ca. 32 eV, is 0.81 eV with the maximum deviation of 1.1 eV. The agreement is fairly good and it provides a justification of our assumption that the angle dependence of the ζ factor, Eq. (9), can be neglected.

4. Sputtering simulation

When interatomic potentials become available, performing MD simulations is mostly a routine work. The methodology of the sputtering simulation was elucidated in paper I. While our simulation method is basically a collection of standard MD techniques, characteristic feature includes the use of NPE rather than NVE dynamics and the use of 3- rather than 2-D periodic boundary conditions. The MD program has been developed by modifying a general-purpose commercial code named GEMS/MD [8].

Table 1 lists the conditions of the simulation. Incident angle is fixed at 0° , 30° , 45° , 60° , and 75° , within a random fluctuation of less than 2° . We ran 50 or 150 separate dynamics for each incident angle, the fewer 50 run applied only to normal incidence. The total number of dynamics runs for each type of the simulation in Table 1 is 650, yielding 2600 as the total sum of the dynamics runs carried out for the present work. Time duration of each dynamics run was 0.5 ps. The time increment Δt used in the integration of the equations of motions was initially chosen by the condition $\Delta t v_0 \leq 0.02 \text{ \AA}$, where v_0 is the incident velocity. After thermalization, Δt was set to 0.2 and 0.32 fs in the D and He bombardment, respectively. Interatomic forces were truncated at 6 Å.

5. Results and discussion

Angle dependence of the sputtering yield is shown in Figs. 3 and 4 for the He and D bombardment, respectively. In these figures, Monte Carlo simulation results by TRIM.SP [9] are also plotted. A significant feature of the MD results in Fig. 4, the He bombardment, is the difference in the yields of the different surfaces. This feature was already observed with respect to the self-sputtering in paper I. A novel feature is that the relative

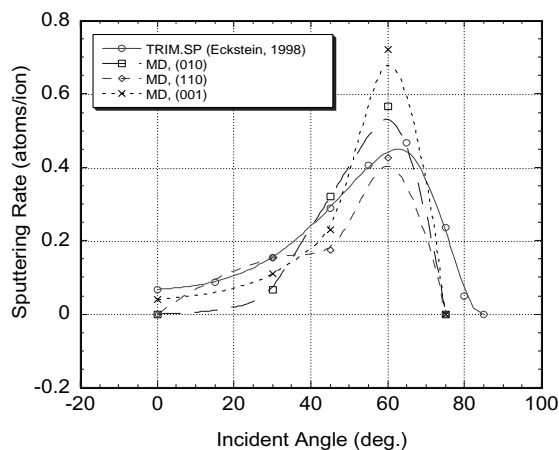


Fig. 3. Incident angle dependence of the sputtering yield for He bombardment (incident energy = 100 eV).

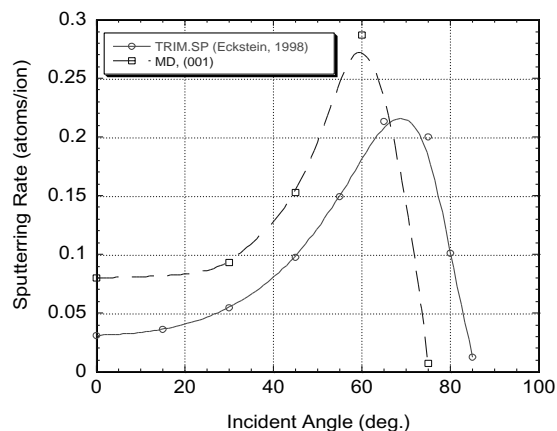


Fig. 4. Incident angle dependence of the sputtering yield for D bombardment (incident energy = 100 eV).

order of the sputtering yield among the different surfaces varies with the incident angle in the present case. Comparing the sputtering yield of the (001) face and (010) face, the former is generally larger than the latter except at 45° . The tendency was opposite in the self-sputtering where the (010) face showed consistently higher sputtering yield than the (001) face. Therefore, it is concluded that the relative susceptibility of different surfaces to the sputtering can change with the incident particle species.

In Figs. 3 and 4, agreement between the MD and TRIM.SP results are generally reasonable. Though the MD results are consistently higher than the TRIM.SP results in the D bombardment, we feel that the deviation of this magnitude is minor considering the complexity involved in the development of the interaction potentials. In fact, we obtained sputtering yields about three

times as large as the present results in an early attempt, where we faithfully followed the original Tersoff formalism including Eqs. (12). The problem in Eqs. (12) is that they tend to give rise to a false many-body effect at short interatomic separations. As seen from Eq. (6), the b factor, the origin of the many-body effect, scales the f_A potential uniformly at all distances. Consequently, large (and false) many-body effect arises at short distances when f_A is an exponential function with large B ($B = 721.37$ eV in the early attempt). Such false effects can be avoided or at least suppressed by using Eq. (13) with which the f_A potential flattens at short distances. As for the deviation of the MD and TRIM.SP sputtering yields in Fig. 4, further investigation is desirable with respect to both the interaction potential and the surface dependence.

6. Concluding remarks

We have presented an MD study of He–Be and D–Be sputtering in the present paper. Combined with paper I where Be self-sputtering was investigated, basic features of the sputtering approached by the atomistic MD simulation have become clear. Firstly, special attention must be paid to the interatomic potentials with respect to the behavior at short distances. This point was stressed in paper I and again have shown up here in relation to the Tersoff potential. A lesson learnt is that potentials developed in other area often need special adaptation when transplanted to the sputtering simulation.

Second characteristic feature to the MD approach is the surface (crystal face) dependence of the sputtering yield. On one hand, this is an advantage of the MD approach that can supply data in any details. On the

other hand, this effect causes a complication in the evaluation of sputtering yields. It is now clear that formulating a method to average sputtering yields of different surfaces is important in establishing the MD approach as a useful tool of the sputtering evaluation. Other characteristic features of the MD approach include the predictions at grazing angles that are in sharp contrast to the TRIM.SP predictions.

Acknowledgements

The authors would like to appreciate Dr Y. Seki, Vice Director of Fusion Engineering Department and Dr Ushigusa, Manager of Reactor System Laboratory, Japan Atomic Energy Research Institute for their great support in this work.

References

- [1] J. Roth, W. Eckstein, M. Guseva, *Fus. Eng. Des.* 37 (1997) 465.
- [2] S. Ueda, T. Ohsaka, S. Kuwajima, *J. Nucl. Mater.* 258–263 (1998) 713.
- [3] D.E. Harrison, *J. Appl. Phys.* 52 (1981) 1499.
- [4] R.A. Chiles, C.E. Dykstra, *J. Chem. Phys.* 74 (1981) 4544.
- [5] R.A. Chiles, C.E. Dykstra, *Chem. Phys. Lett.* 85 (1982) 447.
- [6] W.J. Hehce, L. Radom, P. Schleyer, J.A. Pople, *Ab Initio Molecular Orbital Theory*, Wiley, New York, 1986 (developed and distributed by Wavefunctions).
- [7] J. Tersoff, *Phys. Rev.* 39 (1989) 5566.
- [8] Written by S. Kuwajima and commercially distributed by NanoSimulation Associates.
- [9] W. Eckstein, Report IPP 9/117, 1998.